Induced Crystallization of EVA Having Various VA Contents by Compressed CO_2

Yeong-Tarng Shieh, Yen-Gu Lin

Department of Chemical Engineering, National Yunlin University of Science and Technology, Yunlin 640, Taiwan

Received 28 November 2001; accepted 5 June 2002

ABSTRACT: The crystallization induced by compressed CO_2 was investigated for rubbery ethylene-vinyl acetate copolymer (EVA) containing various amounts of vinyl acetate (VA). The induction of crystallization was demonstrated by appearance of shoulder-like differential scanning calorimetry (DSC) endotherms at temperatures lower than T_m of polyethylene segments of EVA after CO_2 treatments. The intensity of the endothermic shoulders and the degree of crystallinity increased with increasing VA content, suggesting that the interaction of CO_2-carbonyl groups governed the induction of crystallization of EVA upon CO_2 treatment. The interaction of CO_2-carbonyl group was found to decrease with increasing temperature as demonstrated by the decreased crystallization enhancement for 37°C as compared with that for 32°C. The enhancement of crystallization did not monotonically increase with increasing CO_2 pressure, resulting from the interplay of thermodynamic and kinetic driving forces, both being associated with the CO_2 pressure and thus the sorption concentration. © 2002 Wiley Periodicals, Inc. J Appl Polym Sci 87: 1144-1151, 2003

Key words: differential scanning calorimetry; crystallization; infrared spectroscopy

INTRODUCTION

Polymers that can crystallize are seldom in thermodynamic equilibrium; their crystallinities are kinetically affected by treatment conditions. Exposure to liquid or vapor environments that causes crystallization to occur has been reported for some polymers such as poly(ethylene terephthalate)[1–4] and polycarbonate.[5,6] The course of the induced crystallization involves the processes of sorption and diffusion of the diluent into the polymer, leading to plasticization that increases the rate of polymeric segmental motions so that rearrangement into crystals is kinetically possible.[7]

Sorption or dissolution of carbon dioxide (CO_2) in polymers or polymers in carbon dioxide has attracted many researchers[8–18] to study because the environmentally friendly carbon dioxide (especially the supercritical state carbon dioxide) is a potential candidate to be an alternative to substitute for organic chemicals used in modification and processing of polymers, such as using CO_2 as a solvent for polymer synthesis,[19–21] for polymer precipitation by expansion from supercritical solutions,[22–24] for polymerization reactions within CO_2-swollen polymers,[25,26] for separations and fractionations.[27,28] All these uses are associated with interactions between CO_2 and polymers. In addition to other factors such as morphology of polymer, these interactions affect the solubility of CO_2 in polymers or polymers in CO_2, considerably depending on the types of polymers and the CO_2 conditions.

Fourier transform infrared (FTIR) spectroscopy has been used to investigate the interactions of CO_2 with polymers.[29–32] Eckert and co-workers[32] used the bending mode (ν_2) of CO_2 at near 660 cm^{-1} to probe interactions of CO_2 with polymers containing carbonyl groups. Based on the observation of the splitting of this ν_2 band, polymers containing carbonyl groups act as an electron donor and exhibit a specific intermolecular interaction with CO_2 acting as an electron acceptor rather than as an electron donor. Johnston and co-workers[33] have also found that the interaction of CO_2 with polymers possessing acrylate groups (containing carbonyl groups) may be of a Lewis acid–base nature.

In this article, we study the effect of the absorbed CO_2 in EVA (ethylene-vinyl acetate copolymer) via the interaction of CO_2-carbonyl group on the crystallization of EVA containing various amounts of VA (vinyl acetate). The EVA foam prepared by incorporating with CO_2 is a very important material in the shoe industry. The revelation of the CO_2 effect on the crystallization of EVA helps determine the processing conditions of EVA foam to give a finished product with an improved mechanical property.

EXPERIMENTAL

Materials

Four types of EVA including EVA16, EVA18, EVA25, and EVA28 were used as received in a form of cylin-

Correspondence to: Y-T. Shieh (shiehy@pine.yuntech.edu.tw).
Contract grant sponsor: National Science Council of Republic of China.

TABLE I
The VA Contents of the Four EVA Samples Determined by ^{1}H-NMR

Sample code	Weight fraction	Mole fraction
EVA 16	18.24	6.77
EVA 18	18.77	7.00
EVA 25	25.57	10.06
EVA 28	27.11	10.80

drical pellets with a diameter ~4 mm and an axial length ~2.2 mm. EVA16 was supplied by USI Far East Corporation (Taipei, Taiwan) having a trade name UE630, a melt index 1.5 g/10 min, and a density 0.937 g/cm^3. EVA18 was supplied by DuPont Corporation having a trade name EVA460, a melt index 2.5 g/10 min, and a density 0.941 g/cm^3. EVA25 was supplied by USI Far East Corporation having a trade name UE659, a melt index 2.0 g/10 min, and a density 0.947 g/cm^3. EVA28 was supplied by Exxon Corporation having a trade name UL00328, a melt index 3.0 g/10 min, and a density 0.955 g/cm^3.

^{1}H-NMR analyses

The VA contents in EVA samples were determined by means of ^{1}H-NMR (Bruker AMX 400, 400 MHz, $CDCl_3$) using tetramethylsilane as a reference. The assignments of absorption peaks were as follows: 0.92 δ (methyl protons of polyethylene), 1.306 δ (methylene protons of polyethylene), 1.511 δ [methylene protons of poly(vinyl acetate)], 1.9 δ [methyl protons of poly(vinyl acetate)], and 4.917 δ [methine protons of poly(vinyl acetate)]. The VA contents in the four EVA samples can be calculated from the ^{1}H-NMR spectra (not shown in this paper) and are tabulated in Table I.

CO_2 treatments

All four EVA samples used in this study were cylindrical pellets with a volume of ~28 mm^3 for each pellet. The weight of a sample for the CO_2 treatments was ~3.1 g. The CO_2 treatments were performed in a supercritical extractor supplied by ISCO (Lincoln, Nebraska) with a model SFX 2-10 that was equipped with a syringe pump with a model 260D. The samples for the CO_2 treatments were put in a 10-cm^3 cell located inside the extractor pressurized by the equipped syringe-type pump. The extractor was controllable in pressure over the range 0–10,000 psi (680 atm) and in temperature over the range 20–100°C. The pressurizing time for reaching any preset pressure below 680 atm was 30 s. The extractor was controlled at a preset temperature prior to the pressurizing. The exposure (soaking) time for the sample in CO_2 was 1 h, which was experimentally confirmed to be long enough for the cylindrical pellet samples to reach equilibrium sorption. After the exposure, the cell was depressurized to ambient pressure in 10 s and the sample was taken out for weighing in another 10 s to determine the sorption amount. The sample was then left at room temperature until CO_2 inside the sample was fully outgassed as proved by negligible weight change, followed by being subjected to DSC measurements. For FTIR measurements, film samples were cast from chloroform solution and used for the CO_2 treatments.

DSC analyses

A differential scanning calorimeter (DSC2010, TA Instruments, New Castle, DE) was used for determining heating endotherms and cooling exotherms, which were obtained from the same scanning rate of 10°C/min between −60 and 150°C, for EVA samples for before and after CO_2 treatments. The temperature reading and energy involved in DSC thermograms were calibrated with indium (mp 156.6°C, ΔH_f = 6.8 cal/g) and tin (mp 231.88°C, ΔH_f = 14.45 cal/g). The percent crystallinity for the samples was determined by the ratio $\Delta H_m/\Delta H_{m100}$, where ΔH_m was the heats of fusion in joule per gram polyethylene segments in the EVA samples and ΔH_{m100} was the heat of fusion in joule per gram pure polyethylene with 100% crystallinity. The ΔH_m was obtained from the integration of the endothermic peak from the starting of melting (e.g., ~50°C for EVA16 in Fig. 2) to the ending of melting (e.g., 96°C for EVA16 in Fig. 2). The ΔH_{m100} is 281 joule per gram pure polyethylene with 100% crystallinity.[34] Poly(vinyl acetate) segments in the EVA copolymer was assumed to be noncrystalline in the calculation of the percent crystallinity of the sample. The heat of crystallization (ΔH_c) was obtained from the integration of the exothermic peak from the starting of crystallization (e.g., 75°C for EVA16 in Fig. 1) to the ending of crystallization (e.g., ~25°C for EVA16 in Fig. 1).

FTIR analyses

Fourier transform infrared spectrometer (Bio-Rad FTIR, FTS 155) with a resolution of 2 cm^{-1} was used to analyze the CO_2 antisymmetric stretching mode (ν_3) at near 2340 cm^{-1} and the CO_2 bending mode (ν_2) at near 660 cm^{-1}.

RESULTS AND DISCUSSION

As tabulated in Table I, the VA contents of EVA samples, determined by ^{1}H-NMR analyses, are 10.80, 10.06, 7.00, and 6.77 mol % for EVA28, EVA25, EVA18, and EVA16, respectively. The contents of carbonyl groups of samples, thus, are in the order of EVA28 > EVA25 > EVA18 > EVA16 since one mole of vinyl acetate has one mole of carbonyl group. The DSC

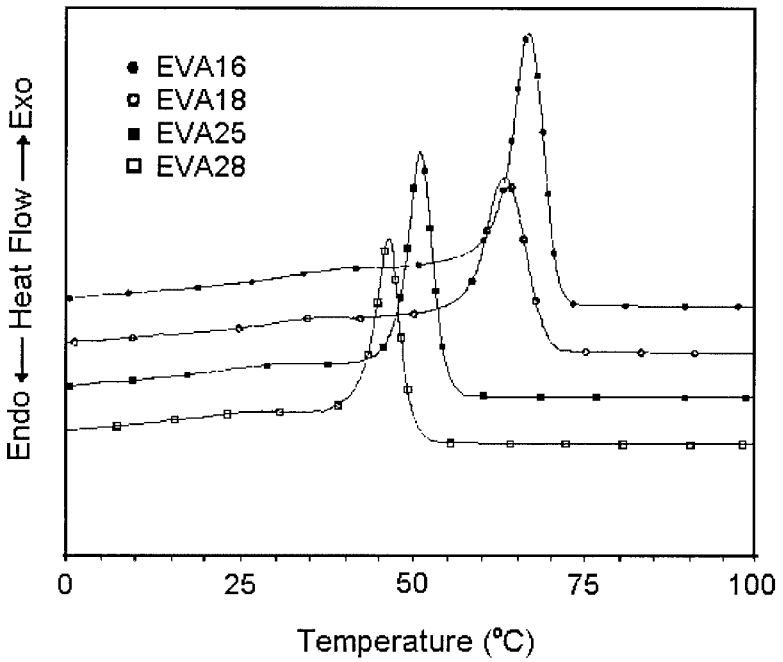

Figure 1 The DSC exotherms of the first cooling scans for EVA samples before CO_2 treatments.

exotherms of the first cooling scans and endotherms of the second heating scans for four samples before CO_2 treatments are shown in Figures 1 and 2, respectively. The exotherms and endotherms arise from the crystallization and melting, respectively, of the polyethylene segments in EVA, since the poly(vinyl acetate) segments in EVA are not crystallizable. The heats of crystallization and fusion calculated by integrating the exothermic and endothermic peaks, respectively, are tabulated in Table II for all four samples. Table II also lists the melting temperatures (T_m), the degrees of crystallinity (X%), and the crystallization temperatures (T_C). The T_m, X%, and T_C in Table II all decrease with increasing VA content in EVA sample, an indication that the acetate groups can impede the crystallization.

Figure 3 presents the DSC endotherms of heating scans for four samples studied after CO_2 treatments at 204 atm and 32°C for 1 h. From these endotherms, although the position of the peaks is insignificantly altered by CO_2 treatments as compared with those untreated as shown in Figure 2, shoulder-like endo-

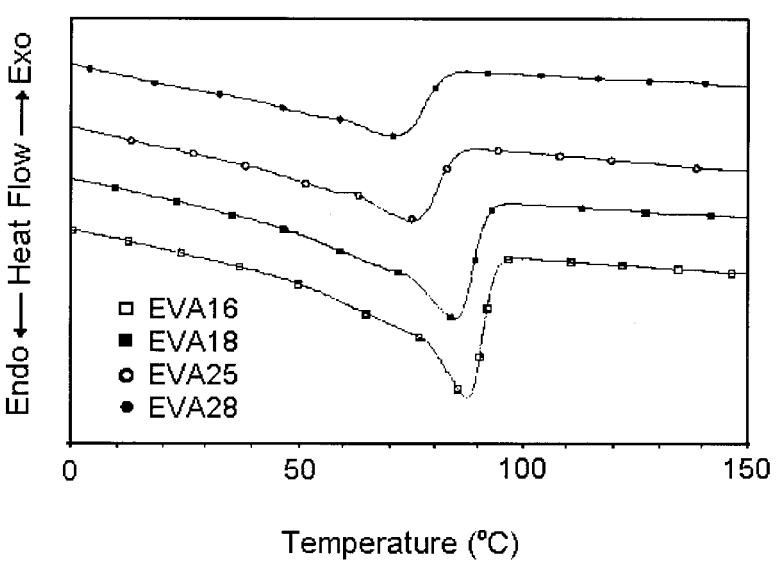

Figure 2 The DSC endotherms of the second heating scans for EVA samples before CO_2 treatments.

TABLE II
Crystallization Temperatures (T_c), Heats of Crystallization (ΔH_c), Melting Temperatures (T_m), Heats of Fusion (ΔH_m), and Degrees of Crystallinity (X%) for Four EVA Samples Before CO_2 Treatments

Sample code	T_c (°C)	ΔH_c (J/g)	T_m (°C)	ΔH_m[a] (J/g)	X%[b]
EVA 16	67.8	100.7	87.9	62.3	27.1
EVA 18	64.1	90.0	85.3	55.6	24.4
EVA 25	52.0	68.8	76.3	35.1	16.8
EVA 28	47.3	59.8	72.9	29.1	14.2

[a] The heat of fusion in joule per gram of sample. The value is divided by the weight fraction of polyethylene segment in EVA to obtain the heat of fusion in joule per gram polyethylene; e.g., for EVA16, 62.3 J/g EVA16 is divided by 0.8176 (from Table I) to obtain 76.20 J/g polyethylene.

[b] X%, the degree of crystallinity, is calculated by dividing the heat of fusion in joule per gram polyethylene in EVA by 281 J/g, the heat of fusion for 100% crystallinity of pure polyethylene.

therms appear at lower temperatures for the treated samples as in Figure 3. These endothermic shoulders are not observed for the samples annealed at 32°C in air at the atmospheric pressure, demonstrating that crystallization has been induced for all four EVA samples after the CO_2 treatment. The induced endothermic shoulders increase in intensity with increasing VA content, indicating that the induction of crystallization is more significant for the sample involving a higher carbonyl group content. Based on the integration of the endotherms in Figure 3, the degrees of crystallinity are calculated and tabulated in Table III. It is clearly demonstrated that the degree of crystallinity increases after CO_2 treatment and that the increase in degree of crystallinity enlarges with increasing VA content. The crystallization of EVA that is induced by CO_2 treatment might arise from the chain mobility of EVA that could be enhanced by the absorbed CO_2. That the increase in degree of crystallinity upon CO_2 treatments enlarges with increasing VA content suggests that the interaction of CO_2-carbonyl group governs the induction of crystallization upon CO_2 treatments, with the higher carbonyl group content leading to the higher CO_2 sorption and thus the higher chain mobility for crystallization. The CO_2 sorption isotherms at 32°C as a function of pressure for all four EVA samples are shown in Figure 4. These sorption isotherms in Figure 4, with the absorbed CO_2 concentration increasing with increasing pressure, can be roughly divided into two pressure regions with the critical pressure (P_c) roughly at the border of the two regions. The absorbed CO_2 concentration for a given pressure is in the order of EVA28 > EVA25 > EVA18 > EVA16. This implies that the sorption capacity of EVA samples is

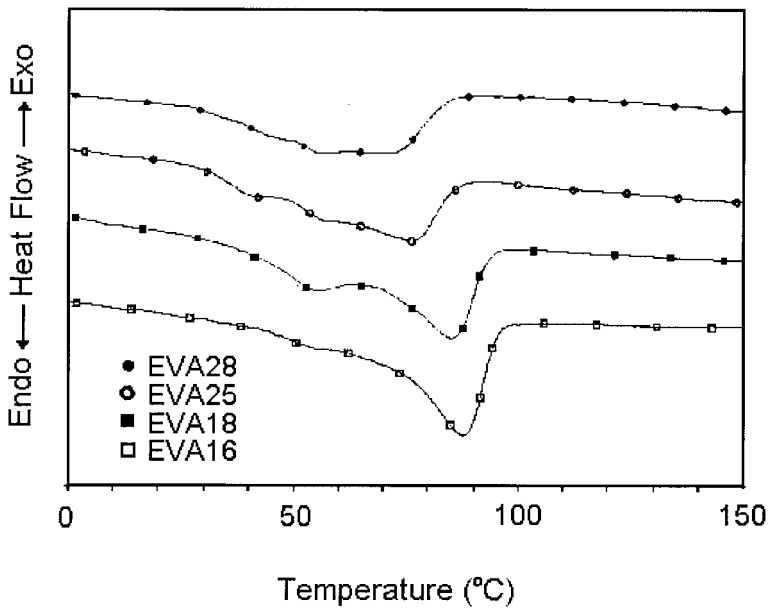

Figure 3 The DSC endotherms of the first heating scans for EVA samples after CO_2 treatments at 204 atm and 32°C for 1 h.

TABLE III
The Increase in Degree of Crystallinity (wt %) for EVA Samples after CO_2 Treatments at 204 atm and Various Temperatures (32 and 37°C) for 1 h

Sample code	VA content (mol %)	32°C	37°C
EVA16	6.77	3.0	0.6
EVA18	7.00	7.1	—
EVA25	10.06	8.6	3.2
EVA28	10.80	9.4	5.9

determined by the contents of carbonyl groups, with the higher carbonyl group content resulting in the higher CO_2 sorption concentration.

The interaction of CO_2-carbonyl group might decrease with increasing temperature as demonstrated by the decreased crystallization enhancement for 37°C as compared with that for 32°C as can be seen from data tabulated in Table III. The existence of the interaction between CO_2 and the carbonyl group can be demonstrated by infrared spectrometric analyses. Figures 5 and 6 present the FTIR spectra for the CO_2 bending mode (ν_2) at near 660 cm^{-1} and the CO_2 antisymmetric stretching mode (ν_3) at near 2340 cm^{-1}, respectively, for EVA28 before and after CO_2 treatments (at 32°C and 204 atm for 1 h) as a function of various desorption times. As can be seen in Figure 5, a single IR absorption band for gaseous CO_2 appears at near 668 cm^{-1} in spectrum f. Three main bands at near 668, 662, and 655 cm^{-1} are evident in the freshly depressurized EVA28-CO_2 film (spectrum e). The two bands at 662 and 655 cm^{-1} that are split from the bending mode (ν_2) of CO_2 are attributed to the interaction of CO_2 with the carbonyl groups of the vinyl acetate, most probably of Lewis acid–base nature.[32] The gaseous CO_2 within EVA28 film having no interaction with the carbonyl groups completely disappears for 2 min of desorption, as demonstrated by the disappearance of the band at 668 cm^{-1} in spectrum d,

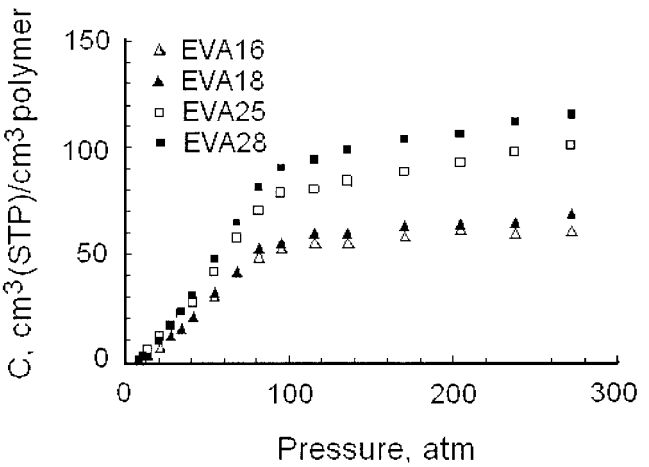

Figure 4 The CO_2 sorption isotherms at 32°C for four EVA samples as a function of CO_2 pressure.

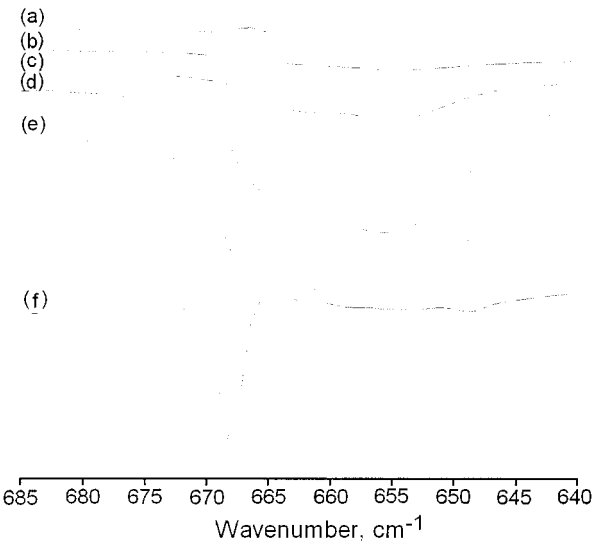

Figure 5 FTIR spectra for the bending mode (ν_2) of CO_2 for (a) EVA28, (f) gaseous CO_2, and the CO_2 entrapped within EVA28 film after (b) 30 min, (c) 5 min, (d) 2 min, and (e) 30 s of desorption.

whereas the CO_2 having interaction with the carbonyl groups does not disappear until 30 min of desorption, as demonstrated by the disappearance of the bands at 662 and 655 cm^{-1} in spectrum b. From spectra b and c in Figure 6, the CO_2 having interaction with EVA28 gives only a band at 2338 cm^{-1} and a weak low-frequency band at 2326 cm^{-1}. That only one band corresponding to the CO_2 ν_3 mode appears in the spectrum suggests that there is only one type of the site within the polymer matrix for the CO_2 molecules under these conditions (desorption times 30 and 5 min). For the freshly depressurized EVA28-CO_2 film or the film with a desorption time of 2 min, gaseous

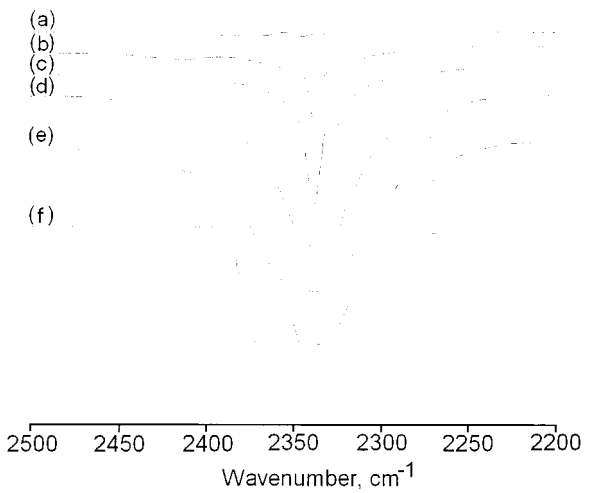

Figure 6 FTIR spectra for the antisymmetric stretching mode (ν_3) of CO_2 for (a) EVA28, (f) gaseous CO_2, and the CO_2 entrapped within EVA28 film after (b) 30 min, (c) 5 min, (d) 2 min, and (e) 30 s of desorption.

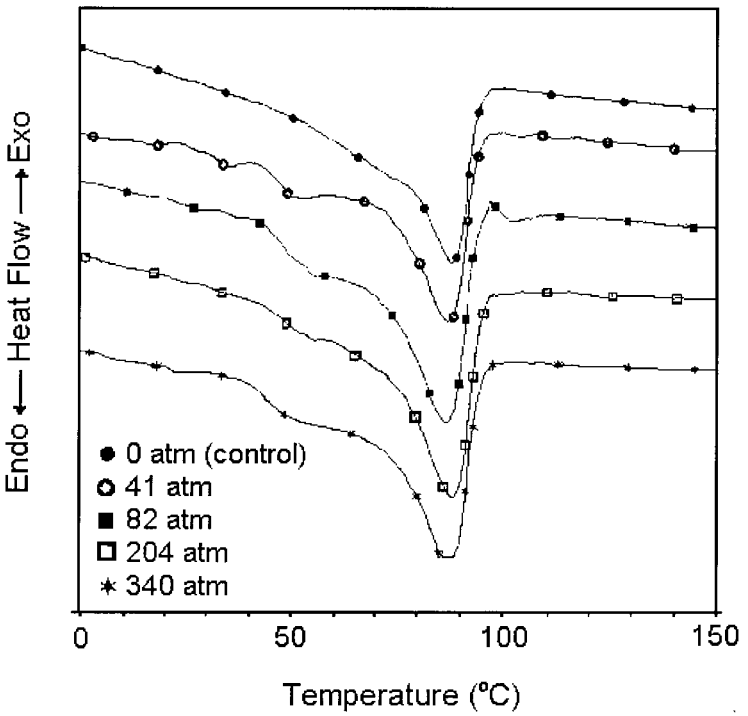

Figure 7 The DSC endotherms of the first heating scans for EVA16 after CO_2 treatments at 32°C and various pressures for 1 h.

CO_2 having no interaction with EVA28 is clearly seen from spectrum d, as demonstrated by the decreasing in absorption intensity of the band at near 2362 cm^{-1}. The width of the 2338 cm^{-1} band increases with increasing amount of CO_2 in EVA28 (as seen from spectrum d), suggesting that various types of the sites

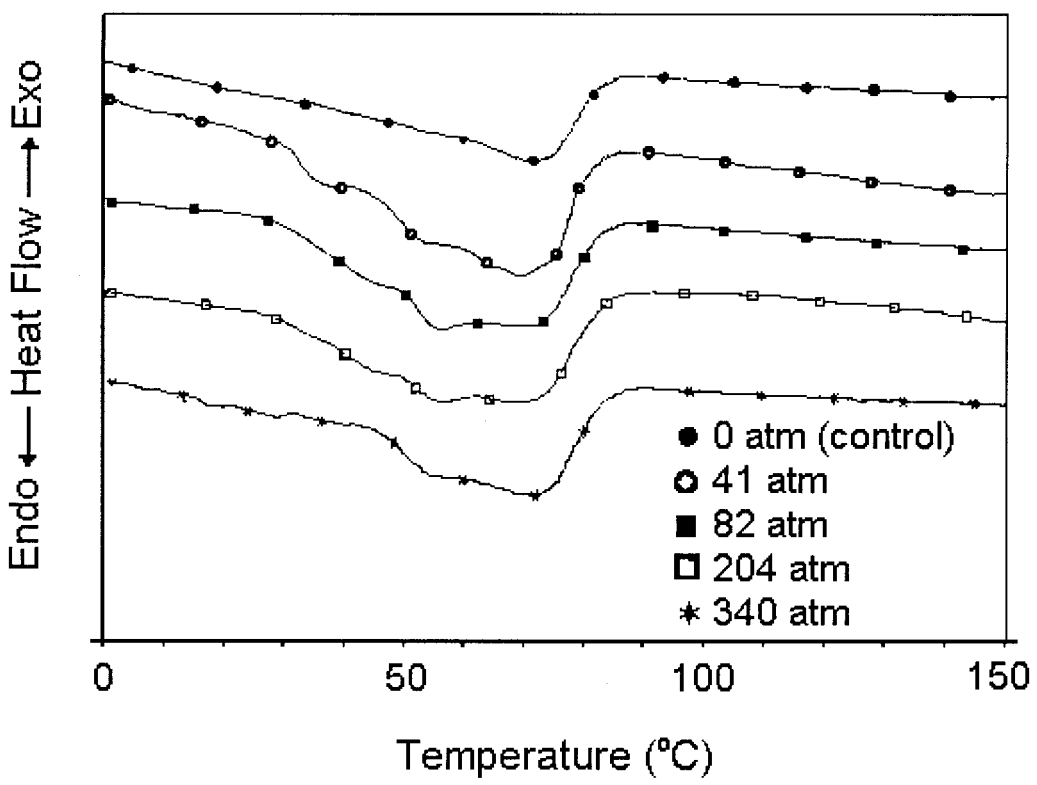

Figure 8 The DSC endotherms of the first heating scans for EVA28 after CO_2 treatments at 32°C and various pressures for 1 h.

TABLE IV
Melting Temperatures (T_m), Heats of Fusion (ΔH_m), and Degrees of Crystallinity (X%) for EVA16 and EVA28 after CO_2 Treatments at 32°C and Various Pressures for 1 h

	T_m (°C)		ΔH_m[a] (J/g)		X%[b]	
Treatment Pressure (atm)	EVA16	EVA28	EVA16	EVA28	EVA16	EVA28
0 (control)	87.9	72.2	62.3	29.1	27.1	14.2
41	86.8	70.7	62.4	56.7	27.1	27.7
82	86.5	71.3	74.2	51.3	32.3	25.1
204	88.0	71.2	69.3	48.3	30.1	23.6
340	87.8	72.0	65.2	36.6	28.4	17.9

[a] As defined in Table II.
[b] As defined in Table II.

within the polymer matrix are present for the CO_2 molecules for those samples having a short desorption time.

Figures 7 and 8 present the DSC endotherms of heating scans for EVA16 and EVA28, respectively, after CO_2 treatments at 32°C and various pressures for 1 h. As can be seen in these two figures, shoulder-like endotherms appear at lower temperatures for all samples after CO_2 treatments, with the intensity varying with treatment pressures. The melting temperatures, heats of fusion, and the calculated degrees of crystallinity for samples for untreated and treated are tabulated in Table IV. The degrees of crystallinity are found to increase for these two samples upon CO_2 treatments at any pressure studied, although the melting temperatures are not clearly altered by the treatments. The obtainable biggest increases in degrees of crystallinity are 13.5 and 5.2% (calculated from Table IV) for EVA28 and EVA16 after treated in CO_2 at 41 and 82 atm, respectively. The degree of crystallinity is not, however, monotonically increasing with increasing treatment pressure, suggesting that multiple factors affect the induction of crystallization upon CO_2 treatments. At low pressures, the extent of the increase in degree of crystallinity increases with increasing pressure resulting from the chain mobility increasing with increasing pressure due to increasing CO_2 sorption (Fig. 4). At high pressures, the chain mobility, however, is too high due to too much CO_2 sorption to provide a thermodynamically stable situation for the crystallization. As a result, the increase in degree of crystallinity is not monotonically increasing with increasing pressure in the high-pressure region. Due to a higher VA content for EVA28 than for EVA16, the absorbed CO_2 amount for EVA28 is higher than that for EVA16 (Fig. 4) so that the destabilization by the absorbed CO_2 for the nucleation for crystallization occurs at a lower pressure, as can be seen from Table IV, where the highest degree of crystallinity is obtained from the 41 atm treatment for EVA28 compared to the 82 atm for EVA16.

CONCLUSIONS

The crystallization of rubbery EVA could be induced by compressed CO_2 as demonstrated by DSC analyses. The enhancement of crystallization was increased with increasing VA content in EVA through the interaction of CO_2 and carbonyl groups. The enhancement of crystallization was decreased with increasing CO_2 treatment temperature, whereas it was increased with increasing CO_2 treatment pressure in a nonmonotonical manner.

We thank the National Science Council of Republic of China for financial support of this work.

References

1. Desai, A. B.; Wilkes, G. L. J Polym Sci, Polym Symp 1974, 46, 291.
2. Jameel, H.; Waldman, J.; Rebenfeld, L. J Appl Polym Sci 1981, 26, 1795.
3. Lin, S. B.; Koenig, J. L. J Polym Sci, Polym Phys Ed 1983, 21, 1539.
4. Chiou, J. S.; Barlow, J. W.; Paul, D. R. J Appl Polym Sci 1985, 30, 3911.
5. Turka, E.; Benechi, W. J Appl Polym Sci 1979, 23, 3489.
6. Ware, R. A.; Tirtowidjojo, S.; Cohen, C. J Appl Polym Sci 1981, 26, 2975.
7. Chiou, J. S.; Barlow, J. W.; Paul, D. R. J Appl Polym Sci 1985, 30, 2633.
8. Barrer, R. M.; Barrie, J. A.; Slater, J. J Polym Sci 1958, 27, 177.
9. Koros, W. J.; Paul, D. R.; Rocha, A. A. J Polym Sci, Polym Phys Ed 1976, 14, 687.
10. Koros, W. J.; Paul, D. R. J Polym Sci, Polym Phys Ed 1978, 16, 1947.
11. Vieth, W. R.; Howell, J. M.; Hsieh, J. H. J Membrane Sci 1976, 1, 177.
12. Michaels, A. S.; Vieth, W. R.; Barrie, J. A. J Appl Phys 1963, 34, 1.
13. Frisch, H. L. Polym Eng Sci 1980, 20, 2.
14. Berens, A. R.; Huvard, G. S. In Supercritical Fluid Science and Technology; Johnston, K. P., Penninger, J. M. L., Eds.; ACS Symposium Series 406; American Chemical Society: Washington, DC, 1989; Chap 14.
15. Kamiya, Y.; Mizoguchi, K.; Naito, Y.; Hirose, T. J Polym Sci, Part B: Polym Phys 1986, 24, 535.
16. Kamiya, Y.; Hirose, T.; Mizoguchi, K.; Naito, Y. J Polym Sci, Part B: Polym Phys 1986, 24, 1525.

17. Fleming, G. K.; Koros, W. J. Macromolecules 1986, 19, 2285.
18. Stern, S. A.; DeMeringo, A. H. J Polym Sci, Polym Phys Ed 1978, 16, 735.
19. DeSimone, J. M.; Maury, E. E.; Menceloglu, Y. Z.; McClain, J. B.; Romack, T. J.; Combes, J. R. Science 1994, 265, 356.
20. Clark, M. R.; DeSimone, J. M. Macromolecules 1995, 28, 3002.
21. Adamsky, F. A.; Beckman, E. J. Macromolecules 1994, 27, 312.
22. Tom, J. W.; Debenedetti, P. G. Biotechnol Prog 1991, 7, 403.
23. Mawson, S.; Johnston, K. P.; Combes, J. R.; DeSimone, J. M. Macromolecules 1995, 28, 3182.
24. Luna-Barcenas, G.; Kanakia, S. K.; Sanchez, I. C.; Johnston, K. P. Polymer 1995, 36, 3173.
25. Watkins, J. J.; McCarthy, T. J. Macromolecules 1994, 27, 4845.
26. Watkins, J. J.; McCarthy, T. J. Macromolecules 1995, 28, 4067.
27. McHugh, M. A.; Krukonis, V. J. Supercritical Fluid Extraction: Principles and Practice, 2nd ed.; Butterworth-Heinemann: Boston, MA, 1994.
28. Paulatis, M. E.; Krukonis, V. J.; Reid, R. C. Rev Chem Eng 1983, 1, 179.
29. Higuchi, A.; Nakagawa, T. J Polym Sci, Part B: Polym Phys 1994, 32, 149.
30. Briscoe, B. J.; Kelly, C. T. Polymer 1995, 36, 3099.
31. Fried, J. R.; Li, W. J Appl Polym Sci 1990, 41, 1123.
32. Kazarian, S. G.; Vincent, M. F.; Bright, F. V.; Liotta, C. L.; Eckert, C. A. J Am Chem Soc 1996, 118, 1729.
33. Mawson, S.; Johnston, K. P.; Combes, J. R.; DeSimone, J. M. Macromolecules 1995, 28, 3182.
34. Brandrup, J.; Immergut, E. H. Polymer Handbook, 3rd ed.; John Wiley & Sons: New York, 1989.